A&A manuscript no.
(will be inserted by hand later)

Your thesaurus codes are:
06 (07.37.2; 19.48.1) 19.58.1;

ASTRONOMY
AND
ASTROPHYSICS
16.4.1998

Spectroscopic discovery of a bipolar jet from the Herbig Ae/Be star LkHα 233*

M. Corcoran[1,2], **T.P. Ray**[2]

[1] Service d'Astrophysiqe, CEA/DSM/DAPNIA/SAp, Centre d'Etudes de Saclay, F-91191 Gif-sur-Yvette Cedex, France
[2] Dublin Institute for Advanced Studies, 5 Merrion Square, Dublin 2, Ireland

Received date ; accepted date

Abstract. We present long-slit [SII]$\lambda\lambda$6716/6731 spectroscopic observations of the Herbig Ae/Be star, LkHα 233. An extended ($\gtrsim\pm5''$) high-velocity ($V_{rad} \sim \pm$ 120kms^{-1}) bipolar Herbig-Haro (HH) jet is detected for the first time. Such jets are rare amongst Herbig Ae/Be stars. While the red-shifted counter-jet is observed to begin 0$''$.7 from the centre of the stellar continuum emission, the blue-shifted jet can be traced right back to the continuum peak. We interpret this asymmetry as being due to the occultation of the counter-jet by a circumstellar disk. Given the distance to LkHα 233, the proposed disk is about 600 AU in radius. The jet, at a position angle of 250°, is perpendicular to the inferred disk orientation based on polarization measurements and bisects the optical bipolar nebula associated with this star.

Close to the star itself ($\lesssim2''$) the [SII]$\lambda\lambda$6716/6731 emission is resolved into 2 velocity components. The high velocity component can be identified with the extended jet, whereas the broad low velocity component is probably a disk wind following the suggestion of Kwan & Tademaru (1995).

Key words: Stars: Pre-Main-Sequence – Stars: Mass Loss – ISM:Jets and Outflows – ISM: Lines and bands

1. Introduction

Optical forbidden emission, such as the [OI]λ6300 line and the [SII]$\lambda\lambda$6716/6731 doublet, has long been used to obtain details of outflows from T Tauri stars (TTS) and Herbig Ae/Be stars (HAEBES). Indirectly they can also be used to infer the distribution of optically thick material around such stars. Appenzeller et al. (1984) and Edwards et al. (1987) were the first to notice that the profiles of the forbidden lines were often asymmetric with the red wing either missing or diminished. They proposed the simple but elegant idea that this asymmetry was due to the receding flow being occulted by an optically thick circumstellar disk. A somewhat naive analysis (see, e.g., Basri & Bertout 1993), based on the emission measure of the forbidden lines, suggested disk sizes, in the case of TTS, of around 100 AU.

Actual forbidden line profiles of young stars can be complex: often two blue-shifted components are present, a high velocity velocity component (or HVC), which can reach velocities of a few hundred kms^{-1} in TTS, and a low velocity component (or LVC), with velocities of perhaps a few kms^{-1} with respect to the systemic velocity of the star (see, e.g., Hartigan et al. 1995). Kwan & Tademaru (1988, 1995) developed a model to explain these double-peaked profiles in which they attributed the high velocity peak to a jet, presumably related to the high velocity jets sometimes observed at greater distances from young stars (e.g. Edwards et al. 1993 or Ray 1996). The low velocity emission is then taken to originate from either a disk wind or disk corona, with the width of the line determined by rotational broadening.

While a sizable number of TTS have double-peaked forbidden emission line profiles (Edwards et al. 1987, Hartigan et al. 1995) the number of HAEBES known with similar characteristics is relatively small. One such object is LkHα 233 (Corcoran & Ray 1997) an A5e pre-main sequence star (d = 880 pc), associated with a bipolar nebula (Herbig 1960; Calvet & Cohen 1978; Staude & Elsässer 1993) having an optical size of about 0.1 pc. The nebula has a distinct X-like morphology with bright reflection limbs at 50°/230° and 90°/270°. While molecular lines are observed towards the star (e.g. Cantó et al. 1984), no molecular outflow has been detected (Leverault 1988). It is a Hillenbrand Group II star (Hillenbrand et al. 1992), and thus has a spectral energy distribution that rises with

Send offprint requests to: M. Corcoran (corcoran@discovery.saclay.cea.fr)

* Based on observations made at the La Palma Observatory and the ESO/MPI 2.2m Telescope, La Silla.

increasing wavelength out to beyond 100μm. Broad band polarimetry carried out on the star and nebula by Aspin et al. (1985) show deviations from a centro-symmetric pattern in keeping with the presence of a large "polarization disk" having an estimated radius of about 15000 AU. The orientation of the "disk" and the position angle of the intrinsic polarization close to the source is about 155° (Vardanyan 1979; Vrba et al. 1979; Leinert et al. 1993). Speckle interferometry, carried out in the near-infrared, (Leinert et al. 1993) shows that the source is surrounded by a light scattering "halo" of about 1″ in size. The polarization of the halo is greater than 10% (at approximately the same position angle as mentioned above) and its discovery prompted Leinert et al. (1993) to suggest that LkHα 233 is highly embedded and optically visible mostly in scattered light. Hamann (1994) found the [FeII] lines in the spectrum of LkHα 233 to be blue-shifted (at about -150 kms^{-1}) with respect to the permitted CaII lines, suggesting the presence of an outflow from this star. Observations by us (Corcoran & Ray 1997) with a randomly oriented slit showed a clear double-peaked profile at both [OI]λ6300 and [SII]$\lambda\lambda$6716/6731. Here we present long-slit spectroscopic observations of LkHα 233 and its immediate environment and observe for the first time an extended optical jet from the star.

2. Observations and Data Reduction

The data presented in this paper were taken in December 1994 at La Palma, using the Intermediate Dispersion Spectrograph (IDS) on the Isaac Newton Telescope. A TEK 3 1280x1180 pixel CCD was employed as the detector and an R1200Y grating used as our dispersing element. The spectral resolution obtained was 0.39 Å/pixel and the spatial resolution 0″.33/pixel. Additional data used in the plot of the extent of the forbidden [SII]$\lambda\lambda$6716/6731 emission (position angle of 226° in Fig. 1) are from a large sample of HAEBES spectra described in Corcoran & Ray (1997).

The long-slit data were reduced using the IRAF[1] long-slit package with bias subtraction, flat field correction, sky subtraction and a wavelength calibration applied. Additionally the stellar continuum was subtracted from the region of interest (here the wavelength range about the [SII]$\lambda\lambda$6716/6731 lines). This subtraction is necessary to increase the contrast of the forbidden emission line region with respect to the background thus providing greater detail close to the star. J. Solf (see, e.g., Böhm & Solf 1994) developed a method of subtracting a model continuum using an appropriate standard star rotationally broadened to match the rotation of the TTS, as used in the observations of TTS by Hirth et al. (1994). Examining a number of standard stars of spectral types A taken at the same time as the HAEBES observations, we note that the photosphere of LkHα 233 should be essentially featureless at ~6716/6731Å and thus no significant contribution from photospheric absorption lines is expected. Therefore, we found it satisfactory to use a simple continuum subtraction method. We fitted each row in the wavelength domain with a low order polynomial, interpolating across the forbidden line region. The continuum image was constructed from the resulting fitted rows. Difference frames (e.g. Fig. 2) produced by subtracting the continuum frame from the original frame, then contain only line emission.

All velocities indicated (e.g. Fig. 2) are with respect to the stellar rest velocity as estimated using the sodium (Na D) interstellar absorption lines (see Corcoran & Ray 1997), and from photospheric iron lines. The typical error in velocity is $\pm$8 kms^{-1}. The positional error is $\pm$0″.3. The results of the observations at various position angles are presented in Table 1, with velocities and extent of the high- and low-velocity components averaged over the two lines of the [SII]$\lambda\lambda$6716/6731 doublet. V_{hvc} and V_{lvc} are the average velocities, relative to the stellar photosphere, of the centroids of the HVC and LVC of the [SII]$\lambda\lambda$6716/6731 lines, respectively. ΔV_{hvc} and ΔV_{lvc} are the full widths half maximum of the HVC and LVC, corrected for instrumental width, in kms^{-1}, as determined by a gaussian fit to each component. The error in the FWHM measurements is $\pm$20 kms^{-1}. Y_f - Y_c is the extent of the forbidden line from the stellar photo-centre measured from the first contour of the forbidden emission above the background 3σ level. [SII]/Hα is the ratio of the [SII] flux to the Hα flux, and is a measure of the degree of shock excitation in the forbidden line forming region.

3. Results and Discussion

While we suspected the presence of a jet from LkHα 233 on the basis of our earlier forbidden line study of this star (Corcoran & Ray 1997), direct narrow-band imaging appeared difficult, especially close to the source, because of the intensity of the associated reflection nebula. Instead several long-slit spectra of LkHα 233 were taken at a range of position angles in an attempt to spectroscopically map the immediate region around the star. We do not reproduce the full set of position-velocity (PV) diagrams here for reasons of space. Fig. 1 shows the variation of extent of the jet and counter-jet with position angle. The complete set of position-velocity diagrams indicate the HH-type jet/counter-jet is at a position angle of of 240-250°/60–70°. This is along the symmetry axis of the bipolar nebula (PA ≈250°) and perpendicular to the polarization angle in the vicinity of the source, i.e. 155° (Vrba et al. 1979; Leinert et al. 1993).

Fig. 2 presents the position-velocity diagram for LkHα 233 along its outflow axis as determined from Fig. 1. Clearly shown are the jet and counter-jet emerging from diametrically opposite sides of this young stellar object.

[1] The IRAF software is distributed by the National Optical Astronomy Observatories under contract with the National Science Foundation

Table 1. Geometry and velocities of the jet/counter-jet from LkHα 233.

Source	P.A. (°)	V_{hvc} (kms^{-1})	V_{lvc} (kms^{-1})	ΔV_{hvc} (kms^{-1})	ΔV_{lvc} (kms^{-1})	Y_f^{hvc} - Y_c ($''$)	[SII]/Hα
LkHα 233	226	-130	-30	80	–	+1.7	0.07
	240	-140	-25	80	180	+2.4	0.06
	247	-125	-15	85	160	+5.0	0.06
	250	-120	-30	85	150	+4.3	0.12
	290	-100	-40	90	160	+1.7	0.07
LkHα 233 (counter-jet)	226	+100	–	60	–	-1.3	0.07
	240	+115	–	55	–	-4.1	0.17
	247	+100	–	80	–	-4.2	0.10
	250	+110	–	55	–	-4.4	0.23
	290	+80	–	95	–	-0.8	0.15

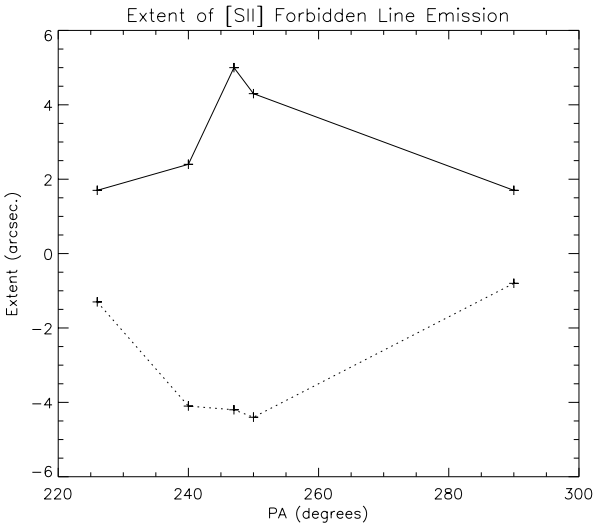

Fig. 1. Spatial extent of the [SII]λ6731 emission in the LkHα 233 jet (solid line) and counter-jet (broken line) as a function of position angle. Greatest extension of the blue and red-shifted forbidden line emission is at position angles ∼ 250° and ∼ 70° respectively. The extent is measured as the first emission line contour above the background 3σ level.

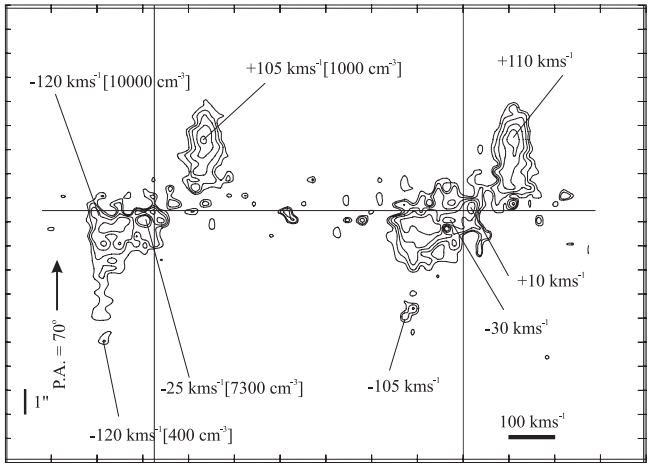

Fig. 2. A position-velocity diagram of LkHα 233 in the region of the [SII]λλ6716/6731 lines. The slit has been oriented along the outflow axis as determined from Fig. 1. The velocities are relative to the stellar rest velocity (vertical lines), electron densities are indicated in square brackets ([ ]), and the spacing of the continuum levels is logarithmic, scaling by factors of $2^{1/2}$. The horizontal line marks the centre of the continuum emission as determined from the fitting procedure (see § 2).

The jet has a maximum blue-shifted radial centroid velocity relative to the velocity of the star (vertical lines) of -140 kms^{-1} and the counter-jet a maximum red-shifted radial centroid velocity of +110 kms^{-1}. Also present is blue-shifted LVC emission but this is seen only close ($\lesssim 2''$) to LkHα 233. The electron densities, as measured from the ratio of the [SII]λ6716/λ6731 lines for a representative temperature of 10^4K, are marked in Fig. 1 in square brackets, at various points along the jet and counter-jet, and are accurate to about ± 20%. Nearer to the star, electron densities are quoted for both the LVC and HVC. Away from the star's position, electron densities can only be measured for the HVC (i.e. the jet and counter-jet). As one would suspect, electron densities are higher closer to the star than further away.

Rather interestingly, the red-shifted counter-jet cannot be traced as close to the stellar photo-centre (horizontal line in Fig. 2) as the blue-shifted jet. Additionally there is a blue-shifted low velocity peak ($V_{lvc} \approx$ -25 kms^{-1}) only seen close to the star. The fact that the low velocity material is blue-shifted and that the red-shifted counter-jet is not seen to reach all the way to the star indicates there is obscuring circumstellar material, presumably a disk, that occludes the initial few tenths of an arcsecond of the re-

ceding outflow. The actual conditions in the counter-jet close the star cannot be determined due to this occultation but it should be remembered that jets and counter-jets often behave differently. The angular separation from the stellar photo-centre to the edge of the counter-jet is $\sim$ 0$''$.7 or slightly more than 600 AU projected on the sky (i.e. a lower limit to its actual extent) at the distance of LkHα 233. Leinert et al. (1993) place an upper limit of 100 AU (FWHM) on the unresolved core they observed using near-IR speckle interferometry and a dimension of about 1$''$ on the "scattering halo" they detected around the star. Clearly the occluding object is not the unresolved core but rather is comparable in size to the scattering halo. The blue-shifted asymmetry of the forbidden emission line region does suggest a disk-like or other flattened geometry, however. Note that the blue-shifted LVC emission is broader than the HVC emission (see also Table 1) and may be modelled (see Kwan & Tademaru 1995) as a rotationally broadened disk wind.

There is a possible over-subtraction of the continuum at the [SII]λ6716 line which may effect the calculated values of the electron densities, N_e, close to the stellar photocentre. Fig. 2 shows that both the HVC and LVC emission at the [SII]λ6716 line is restricted essentially to the western side of the star, unlike the [SII]λ6731 line. If the photospheric spectrum of LkHα 233 is not purely continuum in the region of the 6716Å line, then there may be a problem of over-subtraction during the removal of the continuum. However, no absorption line at that wavelength is visible in the spectra of two spectral standards of types A5II and A7V taken during the same observing run as the LkHα 233 data. As no comparable effect is observed at [SII]λ6731, and the red-shifted counter-jet is observed not to reach the stellar continuum centre in either line, the inference of obscuring circumstellar material is not affected.

Measurements of HH objects and jets associated with lower mass stars (see, for example, Hartigan et al. 1994) show typical ratios of [SII]λ6716+λ6731/Hα $\geq$ 1, indicative of low excitation shocks. In contrast the ratios of [SII]λ6716+λ6731/Hα we find in the LkHα 233 jet and counter-jet are in the range 0.06 – 0.23 (Table 1) and indicate higher excitation shocks. Using the models of Hartigan et al. (1994) we have estimated the corresponding shock velocities to be in the range 50–80 kms^{-1} (see Corcoran & Ray 1997). Interestingly there appears to be a difference between the jet and the counter-jet in that the counterjet seems to be of somewhat lower excitation than the jet itself (see Table 1). Such asymmetries are common amongst bipolar HH jets (e.g. HH 30, Ray et al. 1996). Note also that the velocities, with respect to the systemic velocity of the star, in the counter-jet also also lower, and the line widths probably smaller, than in the jet (see Table 1). Such asymmetries are intrinsic to the flow and must originate close to the source. Their origin, however, is not understood.

In view of the rarity of jets from HAEBES, further studies of this outflow are obviously required. Examples of such studies would include direct narrow-band imaging. Although not used here, direct imaging could be useful in determining the large-scale morphology, and to some degree the history, of the outflow from LkHα 233. Is there, for example, evidence of episodic energetic outbursts in the past? If so then this would indicate that there may be an equivalent of the FU Orionis phenomenon amongst the rarer HAEBES. Spectroscopic studies also of LkHα 233 itself, e.g. of the first overtone bands of CO (Chandler et al. 1993) in the near-infrared, might also show evidence for Keplerian rotation by the innermost regions of the disk indirectly detected here.

Acknowledgements. MC would like to acknowledge funding from Fobairt, the Irish Science and Technology Agency. We would like to express our gratitude to the staff of the La Palma Observatory for their assistance. The Isaac Newton Telescope on the island of La Palma is operated by the Royal Greenwich Observatory at the Spanish Observatorio del Roque de los Muchachos of the Instituto de Astrofisica de Canarias. This research has made use of the Simbad database, operated at CDS, Strasbourg, France.

References

Appenzeller, I., Jankovics, I., & Östreicher, R., 1984, A&A 141, 108
Aspin, C., McLean, I.S., & McCaughrean, M.J., 1985, A&A 144, 220
Basri, G., & Bertout, C., 1993, in: Protostars and Planets III, eds. Levy, E., Lunine, J., University of Arizona Press, p. 543
Böhm, K. -H., & Solf, J., 1994, ApJ 430, 277
Calvet, N., & Cohen, M., 1978, MNRAS 182, 687
Cantó, J., Rodríguez, L.F., Calvet, N., & Leverault R.M., 1984, ApJ 282, 631
Chandler, C.J., Carlstrom, J.E., Scoville, N.Z., Dent, W.R.F., & Geballe, T.R., ApJ 412, L71
Corcoran, M. & Ray, T.P., 1997, A&A 321, 189
Edwards, S.E., Cabrit, S., Strom, S.E., Heyer, I., Strom, K.M., & Anderson, E., 1987, ApJ 321, 473
Edwards, S.E., Ray, T.P. & Mundt, R., 1993, in: Protostars and Planets III, eds. Levy, E., Lunine, J., University of Arizona Press, p. 567
Hamann, F., 1994, ApJS 93, 485
Hartigan, P., Morse, J.A., & Raymond, J., 1994, ApJ 436, 125
Hartigan, P., Edwards, S.E., & Ghandour, L., 1995, ApJ 452, 736
Herbig, G.H., 1960, ApJS 4, 337
Hillenbrand, L.A., Strom, S.E., Vrba, F.J. & Keene, J. 1992, ApJ 397, 613
Kwan, J. & Tademaru, E. 1988, ApJ 322, L41
Kwan, J. & Tademaru, E. 1995, ApJ 454, 382
Leinert, Ch, Haas, M., & Weitzel, N., 1993, A&A 271, 535
Leverault, R.M., 1988, ApJ 330, 897
Ray, T.P., 1996, in NATO ASI Solar and Astrophysical MHD Flows, ed. K. Tsinganos, Kluwer Academic Publishers, p. 539

Ray, T.P., Mundt, R., Dyson, J., Falle, S.A.E.G., Raga, A., 1996, ApJ 468, L103
Staude, H.J., & Elsässer, H. 1993, A&AR 5, 165
Vrba, F.J., Schmidt, G.D., & Hintsen, P.M., 1979, ApJ 227, 185

This article was processed by the author using Springer-Verlag LaTeX A&A style file *L-AA* version 3.